Carcinogenesis vol.27 no.2 pp.245–251, 2006
doi:10.1093/carcin/bgi224
Advance Access publication September 1, 2005

The time and spatial effects of bystander response in mammalian cells induced by low dose radiation

Burong Hu, Lijun Wu*, Wei Han, Leilei Zhang, Shaopeng Chen, An Xu, Tom K.Hei[1] and Zengliang Yu

Key Laboratory of Ion Beam Bioengineering, Institute of Plasma Physics, Chinese Academy of Sciences, Hefei 230031, People's Republic of China and [1]Center for Radiological Research, College of Physicians and Surgeons, Columbia University, New York 10032, USA

*To whom correspondence should be addressed. Tel: +86 551 5591602; Fax: +86 551 5591310;
Email: ljw@ipp.ac.cn

Bystander effects induced by low dose of ionizing radiation have been shown to widely exist in many cell types and may have a significant impact on radiation risk assessment. Though many studies have been reported on this phenomenological observation, the mechanisms underlying this process are not clear, especially on the questions of how soon after irradiation the bystander effects can be initiated and how far this bystander signal can be propagated once it is started. DNA double-strand breaks (DSBs) induced by ionizing radiation or carcinogenic chemicals can be visualized *in situ* using γ-H2AX immunofluorescent staining. Our previous studies have shown that *in situ* visualization of DSBs could be used to assess irradiation-induced extranuclear/extracellular (bystander) effect at an early stage after irradiation. In the present studies, we used this method to investigate the time and spatial effects of damage signals on unirradiated bystander cells. The results showed that increased DSBs in irradiated and unirradiated bystander areas could be visualized 2 min after radiation and reached its maximum 30 min after radiation. The average levels of DSB formation at 30 min post-1cGy irradiation in the irradiated and unirradiated bystander areas were 3-fold and 2-fold higher than those of the sham-irradiated control cells, respectively. Afterwards, the formation of DSBs declined with incubation time and remained steady for at least 6 h at a level that was statistically higher than their controls. The results also showed that the bystander signal derived from irradiated cells could be transferred to anywhere in the dish and the percentage of DSBs in the unirradiated bystander cells was not dependent on the dose delivered. Moreover, the fraction of DSB positive cells in unirradiated bystander areas showed a time-dependent increase based on its distance to the irradiated area at very early stage post-irradiation. Both lindane and DMSO significantly suppressed the yield of DSBs in the cells of unirradiated bystander areas, which suggest that gap junctional intercellular communication and reactive oxygen species played important roles in the induction of the bystander effects, both in irradiated and unirradiated bystander areas.

Abbreviations: DSBs, double-strand breaks; GJIC, gap junctional intercellular communication; MN, micronucleus; RIBE, radiation-induced bystander effects; ROS, reactive oxygen species; SCE, sister chromatid exchange; PCNA, proliferating cell nuclear antigen.

Introduction

The phenomenon known as radiation-induced bystander effects (RIBE) was described almost six decades ago since the earlier work of Kotval and Gray, which showed that α-particles that passed close, but not through the chromatid thread, had a significant probability of producing chromatid breaks or chromatid exchanges in cells (1). The modern day definition of RIBE, however, was derived mainly from the work based on micro-dosimetric principles conducted more than a decade ago by Nagasawa and Little (2), which indicated that an enhanced frequency of sister chromatid exchanges (SCE) was observed in 20–40% of Chinese hamster ovary cells when the culture was exposed to a low dose of α-particles such that only 0.1–1% of the cells' nuclei were expected to be traversed by a particle track. Since then, considerable evidence has accumulated for the existence of these RIBE, in which cells that have not directly been hit by irradiation demonstrate many of the same effects as irradiated cells, using endpoints such as cell killing, micronucleus (MN) induction, mutation, oncogenic transformation and changes in cellular growth pattern (1,3,4). RIBE has been observed in a number of different cell types irrespective of the type of radiation exposure. Both high LET α-particles (5–9) and low LET γ-irradiation (10–12) have been shown to induce RIBE.

While bystander effects have been well demonstrated using a variety of biological endpoints in both human and rodent cell lines, as well as in three-dimensional tissue samples (13), the kinetics and mechanisms of the phenomenon are not clear, especially the time and spatial effects on how the bystander signal is transferred. Belyakov *et al*. reported that there was a 2- to 3-fold increase in the MN level in an unexposed quadrant of the dish, 3 days after 200 cells within one quadrant (5×5 mm^2) of the dish were exposed to α-particles (14). Here, 3 days was chosen as the scoring time that represented the peak formation of micronucleated cells in the population in their studies. Using the ultrasoft X-ray microprobe, available at the Gray Cancer Institute, when only a single V79 cell within the population was targeted, Schettino *et al*. observed that the cell killing occurred among the unirradiated area within a distance of ~3 mm radius from the one targeted cell 3 days after the dishes were revisited (15). Recently, using the bound proliferating cell nuclear antigen (PCNA) in the nuclei of cells as an *in situ* bystander endpoint, Hill *et al*. observed an increase in the expression of PCNA among unirradiated cells in the shielded area of the dish 4 h after irradiation with a 0.4 cGy dose of α-particles (16). There is evidence that bystander cells accumulate phosphorylated (activated) forms of ERK1/2, JNK, p38 and the upstream Raf-1 kinase within 1 min after the cultures are exposed to a mean dose of

5 cGy α-particles (7). Consistent with the occurrence of DNA damage in the irradiated cultures, detectable accumulation of p53 was noted by 15 min after irradiation and an increase in phosphorylation of Ser15 on p53 was also observed by 1 min post-irradiation. Though these studies suggested some kind of time and distance effects of bystander response, the results were estimated based on dosimetric calculation. It is not known, for example, how soon after irradiation the bystander effects can be initiated in the unirradiated bystander area. It is certainly not known how far this signal can be propagated once it is started since the endpoints used in previous studies mostly reflect the phenomenon appearing several hours or several days post-irradiation.

DNA double-strand breaks (DSBs) are considered to be the most relevant lesion for the deleterious effects of ionizing radiation (17,18). One of the earliest steps in the cellular response to DSBs is the phosphorylation of serine 139 of H2AX, a subclass of eukaryotic histone proteins that are part of the nucleoprotein structure called chromatin (19). Using a fluorescent antibody specific for the phosphorylated form of H2AX (γ-H2AX), discrete nuclear foci can be visualized at sites of DSBs *in situ*, either induced by exogenous agents, such as ionizing radiation (20,21), or agents generated endogenously during programmed DNA rearrangements (22–24). Several studies have shown consistently that a γ-H2AX focus represents a DSB and that γ-H2AX foci formation can be used to measure the repair of individual DSBs in human cells (22,24). The induced DSBs are visible as early as 1 min after irradiation (20). The formation of DSBs becomes distinct and reaches the maximum 10–30 min after irradiation, and then decreases to ~30% of this level 1 h later (20). Thus, this *in situ* assay, based on immunochemistry of γ-H2AX, can reflect the early events of damage induced by IR and may provide time-dependent information of bystander effects. Our previous studies demonstrated that *in situ* visualization of DSBs can be used to assess early-stage process of irradiation-induced extranuclear/extracellular (bystander) effects (25).

In the present studies, to analyze the time and spatial effects of the bystander signal transfer and its kinetics at an early stage post-irradiation, we exposed only a part or ~25% of the cells plated onto rectangular dishes (10×6 mm^2, Figure 1) to α-particles. The distances that the bystander signal traveled, together with the degree of the bystander effect on unirradiated cells, were investigated using the DSB assay. The use of rectangular dishes provides an opportunity to divide the non-irradiated area into equal, progressive quadrants from the irradiated area (2.5×6 mm^2).

Materials and methods

Cell culture and alpha-particle irradiation

AG1522 normal human diploid skin fibroblasts, received as a kind gift from Dr Barry Michael (Gray Laboratory, UK), were maintained in α-Eagle's minimum essential medium (Gibco) supplemented with 2.0 mM L-glutamine and 20% FBS (Hyclone) plus 100 μg/ml streptomycin and 100 U/ml penicillin (Gibco) at 37°C in a humidified 5% CO_2 incubator. For irradiation, ~1×10^4 exponentially growing AG1522 cells in passage 11–14 were seeded into each specially designed rectangular dish (internal area: 10×6 mm^2) consisting of a 3.5 μm thick mylar film bottom on which the cells are attached. The culture medium was replaced every 2 days until the cells developed into a confluent monolayer before irradiation. At that time, ~92% of the cells were in G_0–G_1, as determined by flow cytometry. The cells were synchronized in G_0–G_1 by confluent density inhibition of growth to eliminate complications in the interpretation of the results (7). The average energy of α-particles derived from ^{241}Am irradiation source, measured at the cell surface, was 3.5 MeV and the particles were delivered at a dose rate of 1.0 cGy s^{-1}. The dose–response survival curve of AG1522 showed that $D_{37} = 0.317$ Gy and $D_{50} = 0.221$ Gy, when analyzed using the linear-quadratic model (26). During irradiation, 75% of the rectangular dish was shielded using a 100 μm-thick aluminum plate below the dish and cells on the other 25% area were irradiated with the doses of 0, 0.5, 1 and 10 cGy, respectively (Figure 1). Control dishes went through the same irradiation procedure but were 100% shielded. After irradiation, all the dishes were removed to the incubator for 30 min and fixed for immunochemical staining.

To investigate the kinetics of the bystander effects induced in the cells of irradiated and unirradiated areas, and for the analysis of the time-dependent relationships, cells on 25% of the rectangular dish were irradiated with the dose of 1 cGy and then moved to the incubator for the designed time points of 2–360 min before fixing and staining to assess the levels of DSB positive cells.

Treatment with lindane or dimethyl sulfoxide

It has been shown that there are two pathways involved in radiation-induced bystander responses, that is, the pathways involved some medium derived soluble factors, such as short-lived reactive oxygen species (ROS) and those that are mediated by gap junctional intercellular communication (GJIC). To examine the mechanisms underlying the bystander effects accessed by the induction of DSBs in unirradiated bystander areas, all cells in the dish were treated either with 40 μM lindane (Sigma) 2 h before, during and 30 min after irradiation or with 1% (v/v) dimethyl sulphoxide (DMSO) 15 min before, during and 30 min after 25% of the area was irradiated with 1 cGy α-particles. After treatment, cells were fixed 30 min post-irradiation to visualize the levels of DSBs. The dose of the two chemicals used is effective and has previously been shown to be non-toxic and non-genotoxic to the cells under the condition used in present studies (8,27,28).

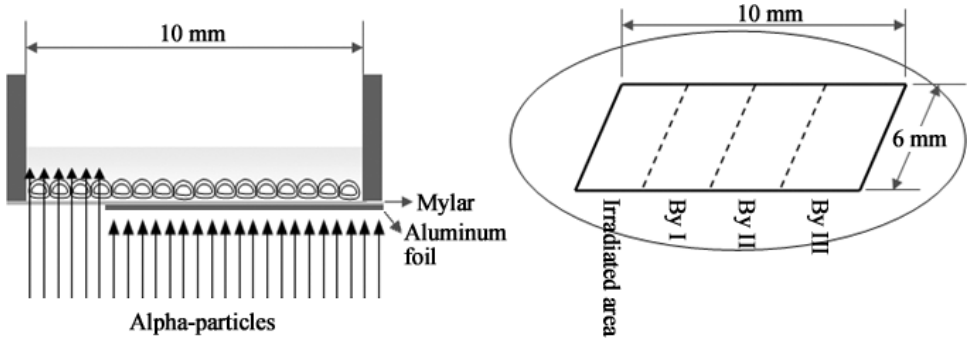

Fig. 1. Schematic diagram of the mylar dish used in the study for irradiation and image capturing. The specially designed dish (internal area: 10×6 mm^2) consists of a 3.5 μm thick mylar film bottom on which the cells are attached. The unirradiated cells were shielded with aluminum (left hand panel). The images were captured in the irradiated area and the unirradiated area, when the mylar dishes containing the stained cells were placed on the 35-mm-diameter glass bottom dish, which was marked and divided equally into four small sections (2.5×6 mm^2) labeled as irradiated area By I, By II and By III corresponding to the rectangular mylar dish (right hand panel).

Immunochemical staining of cells (γ-H2AX) and DSB measurement

Immunochemical staining of cells was performed as described previously (29). Briefly, at a designated time after irradiation, cultures were removed from the incubator, washed with phosphate-buffered saline (PBS) three times, fixed in a 2% paraformaldehyde solution with PBS for 15 min at room temperature and then rinsed three times with PBS again. Prior to immunochemical staining, cells were incubated for 30 min in TNBS solution (PBS supplemented with 0.1% Triton-X 100 and 1% FBS) to improve their permeability and then incubated with anti-γ-H2AX antibody (Upstate Biotechnology, USA) in PBS^+ (PBS supplemented with 1% FBS) for 90 min, washed in TNBS for 3 × 5 min and incubated in PBS^+ containing the FITC-conjugated goat anti-mouse secondary antibody (Sigma) for 60 min. After another wash with TNBS for 3 × 5 min, cells were counter stained using Hoechst33342 (5 μg/ml for 20 min at room temperature). After washing again with TNBS, the stained cells were mounted using 50% of glycerol–carbonate buffer (pH 9.5) for microscopy.

The rectangular mylar dishes containing the stained cells were placed into one 35-mm-diameter glass bottom dish (glass thickness: 0.17 mm, The Netherlands), on which the outline of the rectangular mylar dish was traced and divided equally into four small sections (2.5 × 6 mm^2) corresponding to the rectangular mylar dish (Figure 1). Immunofluorescence images of cells in irradiated and unirradiated areas [labeled as By I (0–2.5 mm), By II (2.5–5 mm), By III (5–7.5 mm to the irradiated area)] were captured using a confocal laser scanning microscope (Lecia, TCS SP2). The captured images on By I area were at least 0.5 mm away from the irradiated area to avoid any secondary scattered particles. Each area was recorded in four images and at least 150 cells in each image were counted. For quantitative analysis, the cells with γ-H2AX foci were regarded as the positive cells and the fraction of positive cells was calculated (cells with DSBs/total cells) (30,31).

Statistical analysis of data

Data were presented as mean and standard deviations from the mean from at least three independent experiments, with at least two replicate dishes per experiment. Significant levels were assessed using Student's *t*-test. A *P*-value of <0.05 between groups was considered to be significant.

Results

Induction of DSBs in irradiated and bystander cells

Approximately 25% of the confluent AG1522 cell monolayers located in one end of the rectangular dishes was irradiated with 0, 0.5, 1 and 10 cGy of α-particles and fixed 30 min after incubation. The γ-H2AX foci, a biomarker for DSBs in the cells, induced by α-particles or generated endogenously, are shown in Figure 2 (white foci in the grey nucleus region of the three-dimensional images). The panels show the tracks representing α-particles traversal and the site of DSBs in the unirradiated bystander area (C), after 10 cGy irradiation (B), and in the sham-irradiated dish (A). Our previous studies, together with others, demonstrated that the DSB formation reached a maximum at 30 min after irradiation with α-particles (19,20,25). Consequently, in the present studies, we chose 30 min as the post-irradiation incubation time to analyze the dose effect on DSB formation in the bystander cells.

Figure 3 shows the fraction of DSB positive cells induced with 0, 0.5, 1 and 10 cGy of α-particles on both the irradiated and unirradiated bystander areas. The fraction of DSB positive cells induced in the irradiated area showed a dose-dependent increase in yield. In cells that were irradiated with a dose of 0.5 or 1 cGy, the fraction of DSB positive cells was 0.363 and 0.422, respectively, in the irradiated area. These yields were significantly greater than those observed in the sham-irradiated cells ($P < 0.01$ for both 0.5 and 1 cGy dose), and also higher than the proportion of cells whose nuclei were estimated to be hit. Based on measured nuclear and cytoplasmic areas of 163 ± 5 μm^2 and 1371 ± 4 μm^2 for the fibroblasts, the percentage of cell nuclei and whole intact cells estimated to be traversed by α-particles was 4.6 or 38.8% for 0.5 cGy and 9.2 or 77.7% for 1 cGy (25). Our previous study has suggested that the cytoplasmic or extranuclear contribution to the increase in DSB foci was minimal (25).

The level of DSB positive cells in unirradiated bystander areas By I, By II and By III all increased 30 min after irradiation. However, the increases were not in a dose-dependent manner, and the average percentages of cells containing γ-H2AX foci in the three unirradiated bystander areas were 0.251, 0.251 and 0.259 for the doses of 0.5, 1 and 10 cGy, respectively. There was no statistically significant difference in the incidence of γ-H2AX positive cells among unirradiated bystander areas. Compared with the sham-irradiation control cells, the increases in DSBs in both the irradiated and in the unirradiated areas were all significantly different ($P < 0.01$). These results are consistent with the published studies using different endpoints (14–16) and suggested that the bystander effects could be induced in unirradiated cells when co-cultured with the irradiated ones.

The time and spatial effects of DSB induction in bystander cells

To detect the time effect of DSB induction, 25% of the confluent AG1522 cell monolayers located in one end of the rectangular dishes was irradiated with a 1 cGy dose of α-particles and the cultures were fixed at a designated time for the immunohistochemical staining of γ-H2AX foci. Figure 4

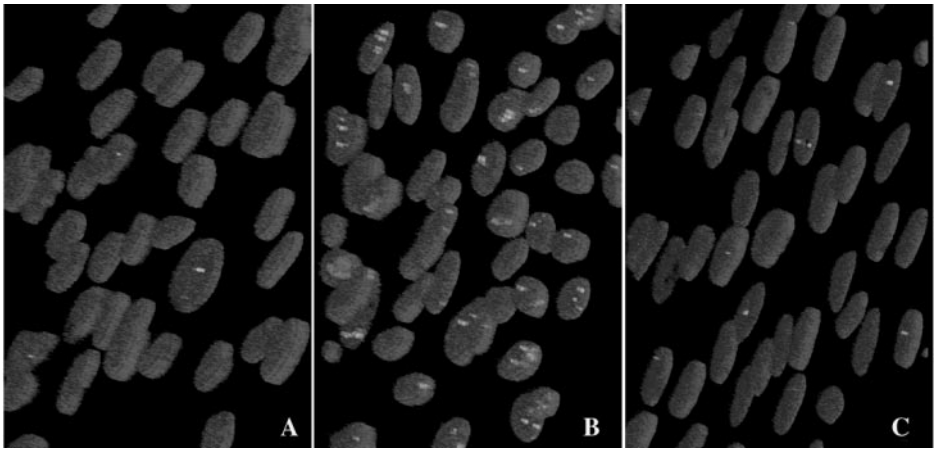

Fig. 2. Induction of DSBs in irradiated and unirradiated bystander cells. Representative image of DSB positive cells (white γ-H2AX foci in the grey nucleus region) in sham-irradiated dish (**A**), 10 cGy α-particle irradiated area (**B**) and bystander area (**C**).

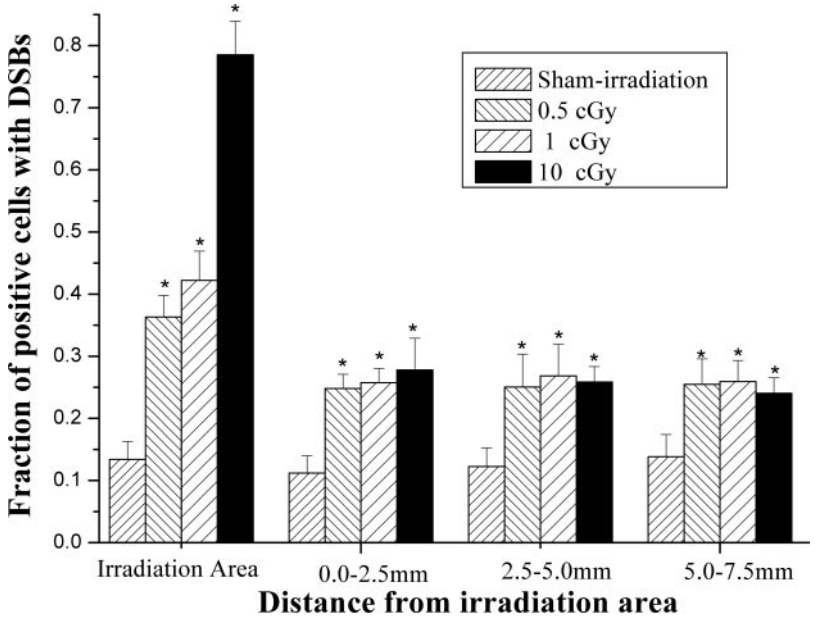

Fig. 3. Induction of DSBs in irradiated and unirradiated bystander fibroblasts. The fractions of DSB positive cells were calculated 30 min after irradiation with 0, 0.5, 1 and 10 cGy of α-particles. Data were pooled from five individual experiments. Error bars represent the standard deviations of the means. Asterisk depicts values that are statistically significant ($P < 0.01$) between the corresponding controls and the experiment groups.

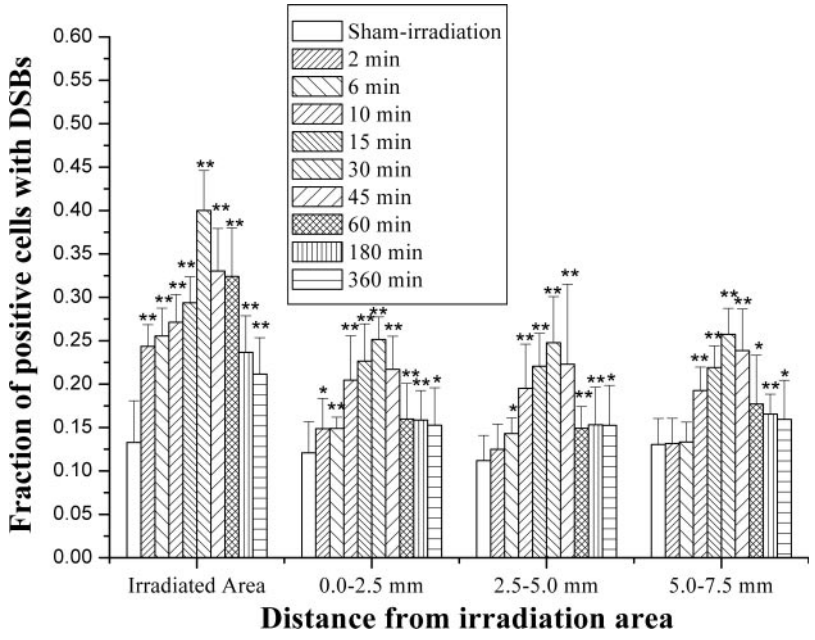

Fig. 4. Bystander DSB induction response as a function of time and distance from irradiated cells in primary human fibroblasts. The fractions of DSB positive cells were calculated 2, 6, 10, 15, 30, 45, 60, 180 and 360 min after irradiation with 1 cGy of α-particles. Data were pooled from three individual experiments. Error bars represent the standard deviations from the means. Asterisks and double asterisks depict values that are statistically significant ($P < 0.05$ and $P < 0.01$, respectively) between the corresponding controls and the experimental groups.

shows that the fraction of induced DSB positive cells in the irradiated area varied with the post-irradiation incubation time and was significantly higher than sham-irradiated controls at all time points examined ($P < 0.01$). By 2 min after irradiation, the fraction of DSBs in By I of the unirradiated bystander area, which is closest to the irradiated section, was already significantly higher than the corresponding sham-irradiated control ($P < 0.01$). In contrast, in By II and By III, no such differences in the fraction of DSBs were detected in 2 min (Figure 4). By 6 min post-irradiation, the percentage of DSBs in both By I and By II showed a progressive increase over the controls, whereas no increase was observed among the bystander cells in By III until 10 min post-irradiation when compared with the corresponding sham-irradiated controls in that zone. From 15 min to the end of the 360 min observational period, when the fractions of DSBs in each zone were monitored, the bystander DSBs in the various unirradiated areas were all significantly higher than the corresponding controls ($P < 0.01$ or $P < 0.05$, as indicated). Furthermore, by 30 min post-irradiation, the incidence of DSBs reached a maximum for both the directly irradiated and bystander cells. With further increase in time, the fractions of DSBs in both irradiated

and unirradiated bystander areas gradually decreased. However, by 360 min post-irradiation, the incidence of DSBs in both of these areas, including the three bystander zones, remained significantly higher than their respective controls.

Attenuation of DSB formation by lindane or DMSO treatment

Pretreatment of cells with either the gap junction communication inhibitor lindane (40 μM) or with the free radical scavenger dimethyl sulphoxide (1%) reduced the fraction of DSB positive cells both in the irradiated and unirradiated bystander areas (Figure 5). In cells irradiated with 1 cGy dose of α-particles, addition of lindane or DMSO reduced the number of cells containing γ-H2AX foci by 48.1 and 56.2% in irradiated area, from 42.2% to 21.9% and 18.5%, respectively ($P < 0.01$). Similar results were also obtained among cells in the three unirradiated bystander areas, and the average decreases were ~32.5% (lindane) and 38.5% (DMSO), from 26.2% to 17.7% and 16.1%, respectively ($P < 0.01$). The decrease in DSB positive cells after treatment with chemical agents suggested that GJIC or ROS might play important roles in the induction of bystander effect, both in irradiated and unirradiated bystander areas.

Discussion

RIBEs have been extensively studied in the past decade (1,3,4). The plethora of data now available concerning this effect fall into two categories: (i) in confluent cultures where physical contacts between irradiated and non-irradiated cells are made and where gap junctional communications have been shown to be essential for the process, and (ii) in sparsely

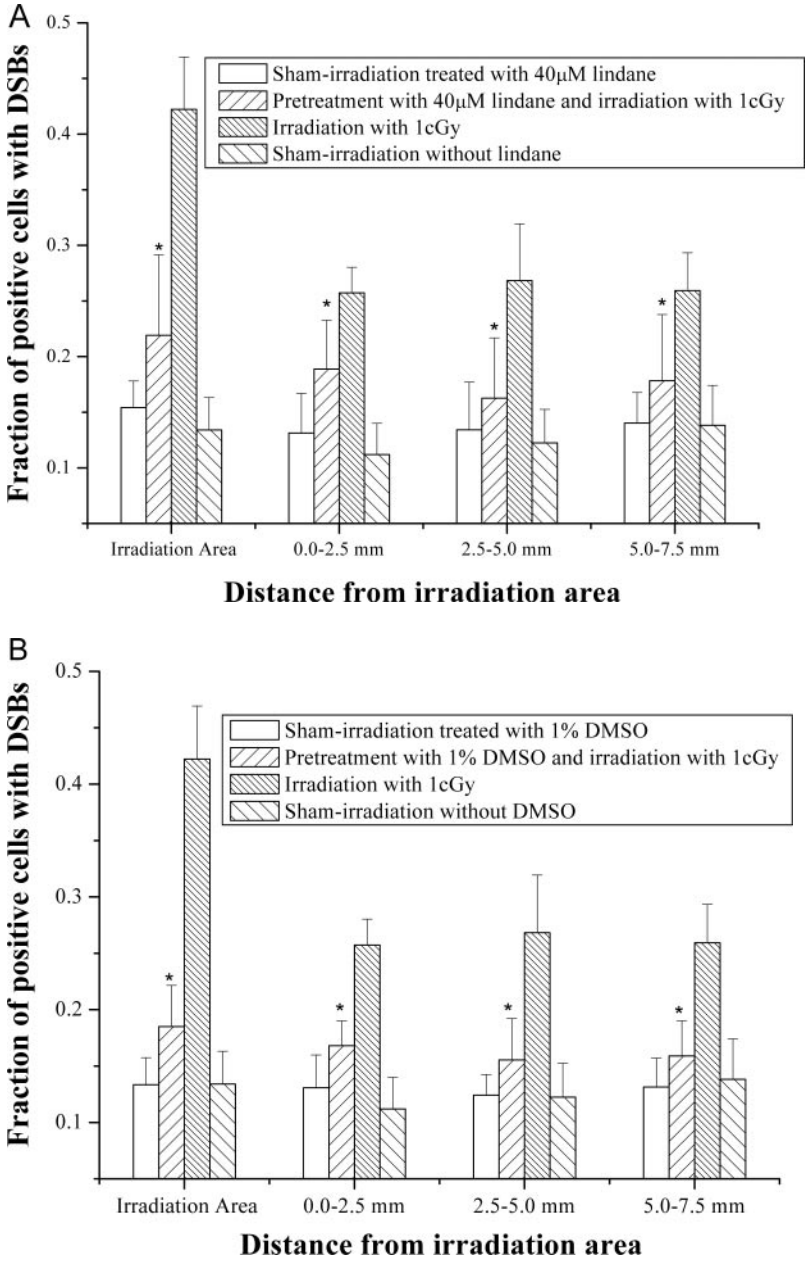

Fig. 5. The fraction of DSB positive cells induced by 1 cGy of α-particle irradiation treated with or without 40 μM lindane (**A**) or 1% DMSO (**B**). Data were pooled from four individual experiments. Error bars represent the standard deviations from the means. Asterisks depict values that are statistically significant ($P < 0.01$) between the lindane or DMSO treated and the untreated groups.

populated cultures where bystander effects may be mediated by damage signals released into the culture medium by the irradiated cells. As a result, incubation of non-irradiated cells with a conditioned medium from irradiated cultures may lead to induction of biological effects. In the present study, confluent monolayers of AG1522 normal human diploid fibroblasts were used. It is not clear whether the signaling molecules involved in the two bystander processes are mutually exclusive. In fact, it is probable that some common initiating or intermediate steps are involved. *In situ* DSB assay, based on the immunohistochemical staining of γ-H2AX, can reflect DSB induction as early as 1 min after irradiation (19,20). Compared with the other endpoints in bystander studies, it provides a fast and real-time method to analyze the transfer of the bystander signal, as well as the kinetics of the RIBE.

Our results from fixing and staining the cells 30 min after irradiation show that the bystander signals initiated by very low doses of α-particles in irradiated cells can induce the DSB damage in the unirradiated bystander cells far away from the irradiated areas (upto 7.5 mm, the longest distance in our experiment system). That is to say, the RIBE can influence any cells in the co-culture dish. This result is consistent with the findings of Belyakov *et al*. (14) and Schettino *et al*. (15), showing that a cell has the same chance of responding to the bystander signals whatever its distance from the irradiated area may be. Moreover, using the *in situ* DSB assay, the average levels of DSB damage in unirradiated bystander areas, after irradiation with the graded doses of α-particles, were found to be ~2-fold higher than that of the controls. No dose-dependent effect was found in unirradiated bystander cells. Such a saturation effect was similar to the findings of Ponnaiya *et al*. (32–34), showing the lack of a dose-dependent response in the induction of MN and chromosomal aberration in unirradiated cells and their progeny.

Our results further demonstrated that the formation of DSBs occurred very soon after irradiation, and the yields of DSB positive cells in both irradiated and unirradiated bystander areas showed a time-dependent increase during the 0–30 min post-irradiation period. Although there is a tendency that a DSB induction decreases after 30 min post-irradiation, the inductions of DSBs at 60, 180 and 360 min post-irradiation are still significantly high than their corresponding controls, and remain steady (Figure 4). The decrease of DSB induction both in irradiated and unirradiated areas 30 min post-irradiation might be due to the repair process initiated in the cells (35,36). There is evidence that after exposure of IMR90 cells to 12 Gy γ-rays, γ-H2AX foci appeared rapidly in 100% of the cell population; in contrast, Rad50 foci appeared more slowly, over a period of several hours (6–8 h post-irradiation) (37). Replication protein A (RPA) plays important roles in DNA replication, repair and recombination. Coincidence of RPA and γ-H2AX foci was detectable at 30 min after irradiation, but the exact coincidence detected at 2 h after γ-rays indicated a time-dependent association of both proteins at the DSB sites (38). Those unrepaired DSBs might be further involved in the induction of SCE, MN, mutation and cancer incidence in the future (39,40). The study of Rothkamm *et al*. (41) also demonstrated that the un-repaired DSBs were induced by low dose γ-irradiation, could persist for days.

It is of interest to observe that at a very early stage (2–6 min) post-irradiation, the induction of DSBs shows a distance-dependent increase, that is, the zone closest to the irradiated area shows the earliest induction of bystander effect (Figure 4). However, 10 min after irradiation, the DSBs induced in the unirradited bystander areas were significantly different from their corresponding controls, and the damaged cells in bystander areas were distributed uniformly over the areas of the dish that was scanned. These results might suggest that the transmission of RIBE is a distance-dependent phenomenon as the bystander signal is propagated across the various zones. To the best of our knowledge, this is the first report that demonstrates the kinetics in the transmission of RIBE.

The mechanism of RIBE, whether involves cell–cell contact or is mediated by soluble factors, is not clear, and is likely to be complex and involve multiple pathways. In sub-confluent cultures, there is evidence that ROS, cytokines such as TGF_{β}, and nitric oxide are essential in mediating the process (1). On the other hand, gap junction mediated cell–cell communications have been shown to be critical in mediating the bystander effects in confluent cultures of either human (27,42) or rodent cells (8,9). In the present study, the results of using lindane, an inhibitor of GJIC, or DMSO, a scavenger of ROS, both of which decreased the fraction of DSB positive cells (Figure 5), both in irradiated and unirradiated bystander areas, suggest that GJIC and ROS might both play important roles in the induction of the bystander effect. It is probable that multiple signaling cascades involving both an initiating event and downstream signaling steps are necessary to mediate the bystander process, and a combination of pathways involving both primary and secondary signaling processes is involved in the bystander process. There is evidence that certain cytokines, such as TGF_{β}, may be involved in the bystander signaling process (43). Recent findings by one of the co-authors have demonstrated that cyclooxygenase-2 (COX-2) signaling cascade plays an essential role in the bystander process. Treatment of bystander cells with NS-398, which suppresses COX-2 activity, significantly reduced the bystander effect (44). It is probable that both radical oxygen species and gap junctional mediated processes contribute to the bystander effects, as indicated by our results.

Acknowledgements

The authors are grateful to Dr Haiying Hang for his technical assistance with DSB detection. This work was funded by National Nature Science Foundation of China under Grant No. 10225526, 30570435 and 30070192, and Grant KSCX2-SW-324 and excellent doctoral thesis foundation of Chinese Academy of Sciences.

References

1. Hei,T.K., Persaud,R., Zhou,H. and Suzuki,M. (2004) Genotoxicity in eyes of bystander cells. *Mutat. Res.*, **568**, 111–120 (review).
2. Nagasawa,H. and Little,J.B. (1992) Induction of sister chromatid exchanges by extremely low doses of alpha-particles. *Cancer Res.*, **52**, 6394–6396.
3. Hall,E.J. and Hei,T.K. (2003) Genomic instability and bystander effects induced by high-LET radiation. *Oncogene*, **22**, 7034–7042 (review).
4. Mothersill,C. and Seymour,C.B. (2004) Radiation-induced bystander effects-implications for cancer. *Nat. Rev. Cancer*, **4**, 158–164 (review).
5. Sawant,S.G., Randers-Pehrson,G., Geard,C.R., Brenner,D.J. and Hall,E.J. (2001) The bystander effect in radiation oncogenesis: I. Transformation in C3H 10T1/2 cells *in vitro* can be initiated in the unirradiated neighbors of irradiated cells. *Radiat. Res.*, **155**, 397–401.
6. Prise,K.M., Belyakov,O.V., Folkard,M. and Michael,B.D. (1998) Studies on bystander effects in human fibroblasts using a charged particle microbeam. *Int. J. Radiat. Biol.*, **74**, 793–798.

7. Azzam,E.I., De Toledo,S.M., Spitz,D.R. and Little,J.B. (2002) Oxidative metabolism modulates signal transduction and micronucleus formation in bystander cells from alpha-particles-irradiated normal human fibroblast culture. *Cancer Res.*, **62**, 5436–5442.
8. Zhou,H., Randers-Pehrson,G., Waldren,C.A, Vannais,D., Hall,E.J. and Hei,T.K. (2000) Induction of a bystander mutagenic effect of alpha particles in mammalian cells. *Proc. Natl Acad. Sci. USA*, **97**, 2099–2104.
9. Zhou,H., Suzuki,M., Randers-Pehrson,G., Vannais,D., Chen,G., Trosko,J.E., Waldren,C.A. and Hei,T.K. (2001) Radiation risk to low fluences of alpha particles may be greater than we thought. *Proc. Natl Acad. Sci. USA*, **98**, 14410–14415.
10. Mothersill,C. and Seymour,C. (1997) Medium from irradiated human epithelial cells but not human fibroblasts reduces the clonogenic survival of unirradiated cells. *Int. J. Radiat. Biol.*, **71**, 421–427.
11. Maguire,P., Mothersill,C., Seymour,C. and Lyng,F.M. (2005) Medium from irradiated cells induces dose–dependent mitochondrial changes and BCL2 responses in unirradiated human keratinocytes. *Radiat. Res.*, **163**, 384–390.
12. Mothersill,C. and Seymour,C. (2002) Bystander and delayed effects after fractionated radiation exposure. *Radiat. Res.*, **158**, 626–633.
13. Bishayee,A., Hill,H.Z., Stein,D., Rao,D.V. and Howell,R.W. (2001) Free radical-initiated and gap junction-mediated bystander effect due to nonuniform distribution of incorporated radioactivity in a three-dimensional tissue culture model. *Radiat. Res.*, **155**, 335–344.
14. Belyakov,O.V., Malcolmson,A.M., Folkard,M., Prise,K.M. and Michael,B.D. (2001) Direct evidence for a bystander effect of ionizing radiation in primary human fibroblasts. *Br. J. Cancer*, **84**, 674–679.
15. Schettino,G., Folkard,M., Prise,K.M., Vojnovic,B., Held,K.D. and Michael,B.D. (2003) Low-dose studies of bystander cell killing with targeted soft X-rays. *Radiat. Res.*, **160**, 505–511.
16. Hill,M.A., Ford,J.R., Clapham,P., Marsden,S.J., Stevens,D.L., Townsend,K.M.S. and Goodhead,D.T. (2005) Bound PCNA in nuclei of primary rat tracheal epithelial cells after exposure to very low doses of plutonium-238 α-particles. *Radiat. Res.*, **163**, 36–44.
17. Hoeijmakers,J.H. (2001) Genome maintenance mechanisms for preventing cancer. *Nature*, **411**, 366–374.
18. Hall,E.J. (1994) *Radiobiology for the Radiologist*, *4th edn*. J.B. Lippincott Company, Philadelphia, Pennsylvania, pp. 16–17.
19. Rogakou,E.P., Pilch,D.R., Orr,A.H., Ivanova,V.S. and Bonner,W.M. (1998) DNA double-stranded breaks induce histone H2AX phosphorylation on serine 139. *J. Biol. Chem.*, **273**, 5858–5868.
20. Rogakou,E.P. and Pilch,D.R. (1999) Megabase chromatin domains involved in DNA double-strand breaks *in vivo*. *J. Cell Biol.*, **146**, 905–915.
21. Burma,S., Chen,B.P., Murphy,M., Kurimasa,A. and Chen,D.J. (2001) ATM phosphorylates histone H2AX in response to DNA double-strand breaks. *J. Bio. Chem.*, **276**, 42462–42467.
22. Chen,H.T., Bhandoola,A., Difilippantonio,M.J., Zhu,J., Brown,M.J., Tai,X., Rogakou,E.P., Brotz,T.M., Bonner,W.M., Ried,T. and Nussenzweig,A. (2000) Response to RAG-mediated VDJ cleavage by NBS1 and gamma-H2AX. *Science*, **290**, 1962–1965.
23. Petersen,S., Casellas,R., Reina-San-Martin,B., Chen,H.T., Difilippantonio,M.J., Wilson,P.C., Hanitsch,L., Celeste,A., Muramatsu,M. and Nussenzweig,A. (2001) AID is required to initiate Nbs1/gamma-H2AX focus formation and mutations at sites of class switching. *Nature*, **414**, 660–665.
24. Mahadevaiah,S.K., Turner,J.M., Baudat,F., Rogakou,E.P., de Boer,P., Blanco-Rodriguez,J., Jasin,M., Keeney,S., Bonner,W.M. and Burgoyne,P.S. (2001) Recombinational DNA double-strand breaks in mice precede synapsis. *Nat. Genet.*, **27**, 271–276.
25. Hu,B., Han,W., Wu,L., Feng,H., Liu,X., Zhang,L., Xu,A., Hei,T.K. and Yu,Z. (2005) *In situ* visualization of DSBs to assess the extranuclear/extracellular effects induced by low dose α-particle irradiation. *Radiat. Res.*, **164**, 286–293.
26. Hu,B., Wu,J., Han,W., Wang,X., Wu,L. and Yu,Z. (2005) Development of a dose-adjustable α-particle irradiation facility for radiobiological studies. *Nucl. Sci. Techn.*, **16**, 102–107.
27. Azzam,E.I., de Toledo,S.M. and Little,J.B. (2001) Direct evidence for the participation of gap junction-mediated intercellular communication in the transmission of damage signals from α-particle irradiated to nonirradiated cells. *Proc. Natl Acad. Sci. USA*, **98**, 473–478.
28. Narayanan,P.K., Goodwin,E.H. and Lehnert,B.E. (1997) Alpha particles initiate biological production of superoxide anions and hydrogen peroxide in human cells. *Cancer Res.*, **57**, 3963–3971.
29. Aten,J.A., Stap,J., Krawczyk,P.M., van Oven,C.H., Hoebe,R.A., Essers,J. and Kanaar,R. (2004) Dynamics of DNA double-strand breaks revealed by clustering of damaged chromosome domains. *Science*, **303**, 92–95.
30. Limoli,C.L., Giedzinski,E., Bonner,W.M. and Cleaver,J.E. (2002) UV-induced replication arrest in the xeroderma pigmentosum variant leads to DNA double-strand breaks, gamma-H2AX formation, and Mre11 relocalization. *Proc. Natl Acad. Sci. USA*, **99**, 233–238.
31. d'Adda di Fagagna,F., Reaper,P.M., Clay-Farrace,L., Fiegler,H., Carr,P., Von Zglinicki,T., Saretzki,G., Carter,N.P. and Jackson,S.P. (2003) A DNA damage checkpoint response in telomere-initiated senescence. *Nature*, **426**, 194–198.
32. Ponnaiya,B., Cornforth,M.N. and Ullrich,R.L. (1997) Induction of chromosomal instability in human mammary cells by neutrons and γ-rays. *Radiat. Res.*, **147**, 288–294.
33. Ponnaiya,B., Jenkins-Baker,G., Brenner,D.J., Hall,E.J., Randers-Pehrson,G. and Geard,C.R. (2004) Biological responses in known bystander cells relative to known microbeam-irradiated cells. *Radiat. Res.*, **162**, 426–432.
34. Ponnaiya,B., Jenkins-Baker,G., Bigelow,A., Marino,S. and Geard,C.R. (2004) Detection of chromosomal instability in α-irradiated and bystander human fibroblasts. *Mutat. Res.*, **568**, 41–48.
35. Rothkamm,K., Krüger,I., Thompson,L.H. and Löbrich,M. (2003) Pathways of DNA double-strand break repair during the mammalian cell cycle. *Mol. Cell. Biol.*, **23**, 5700–5715.
36. Nazarov,I.B., Smirnova,A.N., Krutilina,R.I. *et al.* (2003) Dephosphorylation of histone γ-H2AX during repair of DNA double-strand breaks in mammalian cells and its inhibition by calyculin A. *Radiat. Res.*, **160**, 309–317.
37. Paull,T.T., Rogakou,E.P., Yamazaki,V., Kirchgessner,C.U., Gellert,M. and Bonner,W.M. (2000) A critical role for histone H2AX in recruitment of repair factors to nuclear foci after DNA damage. *Curr. Biol.*, **10**, 886–895.
38. Balajee,A.S. and Geard,C.R. (2004) Replication protein A and gamma-H2AX foci assembly is triggered by cellular response to DNA double-strand breaks. *Exp. Cell Res.*, **300**, 320–334.
39. Petukhova,G., Stratton,S. and Sung,P. (1998) Catalysis of homologous DNA pairing by yeast Rad51 and Rad54 proteins. *Nature*, **393**, 91–94.
40. Fenech,M. (2000) The *in vitro* micronucleus technique. *Mutat. Res.*, **455**, 81–95.
41. Rothkamm,K. and Lobrich,M. (2003) Evidence for a lack of DNA double-strand break repair in human cells exposed to very low x-ray doses. *Proc. Natl Acad. Sci. USA*, **100**, 5057–5062.
42. Shao,C., Furusawa,Y., Kobayashi,Y., Funayama,T. and Wada,S. (2003) Bystander effect induced by counted high-LET particles in confluent human fibroblasts: a mechanistic study. *FASEB J.*, **17**, 1422–1427.
43. Iyer,R., Lehnert,B.E. and Svensson,R. (2000) Factors underlying the cell growth-related bystander responses to alpha particles. *Cancer Res.*, **60**, 1290–1298.
44. Zhou,H., Ivanov,V.N., Gillespie,J., Geard,C.R., Amundson,S.A., Brenner,D.J., Yu,Z., Lieberman,H.B. and Hei,T.K. (2005) Mechanism of radiation-induced bystander effect: role of COX-2 signaling pathway. *Proc. Natl Acad. Sci. USA*, **102**, in press.

Received June 9, 2005; revised August 26, 2005; accepted September 3, 2005